Journal of Power Sources 244 (2013) 505–509

Contents lists available at SciVerse ScienceDirect

Journal of Power Sources

journal homepage: www.elsevier.com/locate/jpowsour

Short communication

Synthesis and electrochemical properties of layered $Li_{1.0}Mn_{0.82}Ni_{0.10}Ti_{0.08}O_2$ prepared by chemical lithium insertion

Naoya Ishida [a,*], Hiroshi Hayakawa [a], Hideka Shibuya [b], Junichi Imaizumi [b], Junji Akimoto [a]

[a] National Institute of Advanced Industrial Science and Technology (AIST), Tsukuba Central 5, 1-1-1 Higashi, Tsukuba, Ibaraki 305-8565, Japan
[b] Tanaka Chemical Corporation, 45-5-10 Shirakata-cho, Fukui-shi, Fukui 910-3131, Japan

HIGHLIGHTS

- We synthesize the $Li_{1.0}Mn_{0.82}Ni_{0.10}Ti_{0.08}O_2$ positive electrode materials using soft-chemical method.
- The initial discharge capacity with lithium anode is 244 mAh g^{-1}.
- They exhibit high coulombic efficiency of 98% at first cycle.
- High capacity, 208 mAh g^{-1}, is confirmed with graphite anode.

ARTICLE INFO

Article history:
Received 30 October 2012
Received in revised form
19 February 2013
Accepted 8 March 2013
Available online 19 March 2013

Keywords:
Lithium ion battery
Positive electrode material
Layered rock-salt type structure
Chemical lithium insertion
Coulombic efficiency

ABSTRACT

The novel $Li_xMn_yNi_zTi_{1-y-z}O_2$ compounds were prepared by Na^+/Li^+ ion-exchange and chemical lithium insertion. The eight products were characterized using X-ray diffraction, ICP-AES, SEM, and electrochemical measurements. All the samples were adopted the layered rock-salt type structure. The electrochemical properties of $Li_{0.6}Mn_{0.82}Ni_{0.10}Ti_{0.08}O_2$ sample exhibited the best capacity retention of 87% at 20th charge–discharge test in the voltage range of 1.5 and 5.0 V of all the present samples. The extra lithium was added by chemical lithium insertion using LiI and then fully occupied $Li_{1.0}Mn_{0.82}Ni_{0.10}Ti_{0.08}O_2$ in lithium site was obtained. The initial charge and discharge capacities of $Li/Li_{1.0}Mn_{0.82}Ni_{0.10}Ti_{0.08}O_2$ cell were 250 mAh g^{-1} and 244 mAh g^{-1}, respectively, with the first coulombic efficiency of 98% between 2.0 and 4.8 V. The graphite/$Li_{1.0}Mn_{0.82}Ni_{0.10}Ti_{0.08}O_2$ cell indicated the first discharge capacity of 208 mAh g^{-1} at 1.8 V after charging up to 4.7 V. The irreversible capacity loss of 39 mAh g^{-1} was ascribed to the formation of a solid–electrolyte interface (SEI). The $Li_{1.0}Mn_{0.82}Ni_{0.10}Ti_{0.08}O_2$ is one of the promising materials for positive electrode material in lithium ion batteries for the view point of high capacity and coulombic efficiency.

1. Introduction

Layered rock-salt type oxides are of interest for the positive electrode materials in secondary lithium ion batteries (LIBs). Especially, the $LiCoO_2$ is the most commercially used material due to its high electric capacity and excellent cycle life [1]. The high cost and toxicity of cobalt compounds, however, have led to the investigation of alternative materials that intercalate lithium ions. So far, the layered rock-salt type $LiNiO_2$ [2], $LiNi_{0.5}Mn_{0.5}O_2$ [3], $LiMnO_2$ [4–6], Li_2MnO_3 [7,8] and Li_2MnO_3–$LiMO_2$ compounds (M = Mn, Co, Ni) [9,10], etc. have been intensively studied. Since the Ni^{2+}ion was suggested to be replaced with Li^+ ion due to similar ionic radii [11], the electrochemical capacity was reduced for Ni-rich positive materials such as $LiNiO_2$, $LiNi_{0.8}Co_{0.15}Al_{0.05}O_2$, and $LiNi_{0.5}Mn_{0.5}O_2$. Although Li_2MnO_3–$LiMO_2$ materials showed quite high capacity, the oxide ion oxidation in the initial charge resulted in low coulombic efficiency [12]. The disadvantage of $LiMnO_2$ was to convert to spinel-type structure on charge–discharge cycling. The phase transformation was suppressed by the partial substitution of the other ions for manganese ion [13–18]. Thus, expectations in regard to the modified Mn-rich $LiMn_yM_{1-y}O_2$ ($y > 0.5$, M = transition metal ion) are fairly high on the high theoretical capacity of ca. 285 mAh g^{-1}.

The soft chemical synthesis method has opened route for the synthesis of layered rock-salt type $LiMnO_2$ that are difficult or impossible to obtain by high temperature solid-state reactions [6,19,20]. The main advantage of such a soft chemical method is to induce the preparation of meta-stable phases and to considerably

* Corresponding author. Tel.: +81 29 861 2843; fax: +81 29 861 9214.
E-mail address: naoya-ishida@aist.go.jp (N. Ishida).

0378-7753/$ – see front matter © 2013 Elsevier B.V. All rights reserved.
http://dx.doi.org/10.1016/j.jpowsour.2013.03.029

reduce the formation temperature. In order to alleviate reaction conditions, environmental impact and decrease the economic cost, the synthesis of this material through soft chemical method would be prior if the properties of the material could be retained. Although we have previously synthesized the layered rock-salt type $Li_{0.55}Mn_{0.5}Ni_{0.25}Ti_{0.25}O_2$ which did not convert to spinel-type structure in electrochemical test, low retention rate was obtained [17]. In this study, the appropriate molar ratio of manganese, nickel and titanium ions in the $Li_xMn_yNi_zTi_{1-y-z}O_2$ compounds is established to improve the electrochemical cycle life.

While the composition of transition metals has been needed to be optimized, fully occupied lithium site has been also required because many studies showed considerable deficiencies of lithium site ($0.5 < x < 0.8$) after Na^+/Li^+ ion-exchange reaction [6,13–15,17,20,21]. In the previous study, the additive lithium ion insertion was performed by reducing LiI and then the extra lithium ion can be inserted in lithium layer [21,22]. In the present study, the $Li_{1.0}Mn_{0.82}Ni_{0.10}Ti_{0.08}O_2$ was first synthesized to combine the Na^+/Li^+ ion-exchange method with the chemical lithium insertion and examined for the electrochemical properties. We report the $Li_{1.0}Mn_{0.82}Ni_{0.10}Ti_{0.08}O_2$ material is one of the attractive materials for the LIBs and gave a high electrochemical capacity and excellent coulombic efficiency.

2. Experimental

$Li_xMn_yNi_zTi_{1-y-z}O_2$ ($x < 0.7$, $0.5 < y < 0.95$, $0.05 \leq z < 0.25$) was prepared via the soft chemical method such as Na^+/Li^+ ion-exchange and chemical lithium insertion. The host materials, $Na_{0.7}Mn_yNi_zTi_{1-y-z}O_2$, were prepared by heating the appropriate molar ratios of $CH_3COONa\cdot 3H_2O$ (Wako Chemicals Co., 99.5% purity) and manganese nickel and titanium hydroxides prepared by a co-precipitation method. They were mixed and then heated at 500 °C in air. For the Na^+/Li^+ ion-exchange, the host materials were refluxed with an 8-fold molar excess of LiBr in ethanol at 80 °C for 6 h. After the reaction, they were then filtered, washed with ethanol and water, and dried at 120 °C for 12 h.

For chemical lithium insertion into Na^+/Li^+ ion-exchanged material, the following treatment was performed. The ion-exchanged $Li_{0.6}Mn_{0.8}Ni_{0.1}Ti_{0.1}O_2$ samples reacted with a two-fold molar excess of LiI in dry acetonitrile to form the $Li_{1.0}Mn_{0.8}Ni_{0.1}Ti_{0.1}O_2$ materials. The condition involved refluxing at 80 °C for 5 h in air. The resulting materials were washed with acetonitrile and vacuum dried at 120 °C for 12 h. Typically, the reaction can be described as follows:

$$Li_{0.6}Mn_{0.82}Ni_{0.10}Ti_{0.08}O_2 + 2LiI \rightarrow Li_{1.0}Mn_{0.82}Ni_{0.10}Ti_{0.08}O_2 + 0.2LiI_3 + 1.4LiI$$

Chemical compositions were determined by inductively coupled plasma atomic emission spectroscopy (ICP-AES, Shimadzu ICPS-8000). X-ray diffraction patterns of the samples were obtained with an X-ray diffractometer (Rigaku RINT2550V: 40 kV, 200 mA) with Cu Ka radiation. The diffraction data were collected for 1 s at each 0.03° step width over a 2θ range 10–90°. The structural parameters were refined with the RIETAN-FP program [23]. The field-emission scanning electron microscopy (FE-SEM, Hitachi, S-4300) was used to characterize the morphology and crystal sizes of obtained materials with or without chemical lithium insertion.

The electrochemical intercalation and deintercalation of lithium ions were carried out using lithium cells. The working electrode was consisted of a mixture of $Li_xMn_yTi_zNi_{1-y-z}O_2$/acetylene black/polytetrafluoroethylene (PTFE) with the weight ratio of 5:5:1. The mixture was cast on an aluminum mesh, pressed, and then dried at 120 °C in vacuum oven. The cells used for electrochemical tests were constructed in a CR2032 coin-type cell. The counter electrodes were selected as a 15-mm diameter of lithium metal foil for lithium cells or a 92/8 wt% graphite/polyvinylidene-difluoride (PVDF) composite film onto Cu foil for full cells. The separator employed was a glass filter sheet and a microporous polypropylene sheet. A solution of 1 M $LiPF_6$ in a 1:1 mixture of ethylene carbonate (EC) and diethylcarbonate (DEC) by volume (Kishida Chemical Co., Ltd.) was used as the electrolyte. All the cells were constructed in an argon-filled globe box and tested at room temperature (25 °C). Charge capacity was measured by constant current and constant voltage (CCCV) mode up to 4.8 V or 5.0 V for lithium anode cells and to 4.7 V for full cell (30 mA g^{-1} and then potentiostatic step for 2 h), while discharge capacity was estimated by constant current mode (30 mA g^{-1}) at 1.5 V or 2.0 V for lithium anode cells and 1.8 V for full cell.

3. Results and discussions

A variety of samples $Li_xMn_yNi_zTi_{1-y-z}O_2$ ($x < 0.7$, $0.5 < y < 0.95$, $0.05 \leq z < 0.25$) were prepared by Na^+/Li^+ ion-exchanging for the appropriate sodium materials, $Na_{0.7}Mn_yNi_zTi_{1-y-z}O_2$ ($0.5 < y < 0.95$, $0.05 \leq z < 0.25$) calcined at 500 °C, and investigated by XRD and ICP-AES. Those samples were characteristic by broad diffraction lines as shown in Fig. 1. All the diffraction lines were indexed in the layered rock-salt type structure (space group of $R\bar{3}m$). Their lattice constants were measured by a least square method using eight diffraction lines. Table 1 gives the sample names, chemical compositions and the lattice parameters of Na^+/Li^+ ion-exchanged products. The first three letters of the sample name identify the initial of transition metal atoms (M = manganese, N = nickel, and T = titanium), followed by about molar ratios in transition-metals (e.g. MNT552025 = Mn: 55%, Ni: 20% and Ti: 25%). Most of sodium in host material was replaced by lithium with residual sodium contents between 0.03 and 0.05 molar ratios. The MNT552025, MNT601525, MNT651025 and MNT700525 samples showed about unity in the Ti/M ratios (0.23–0.24 molar ratios), while the nickel contents, z, were in the range of 0.05 and 0.20. The remaining three samples, MNT701515, MNT801010 and MNT900505, differ from not only nickel contents but also titanium one (Ni + Ti contents ≈ 0.1, 0.2 and 0.3 molar ratios).

Electrochemical properties were compared for different samples (Fig. 2) at 30 mA g^{-1} in the potential range of 1.5–5.0 V versus Li/Li^+. While the MNT552025, MNT601525, MNT651025 and MNT700525 samples tended to decrease the initial discharge

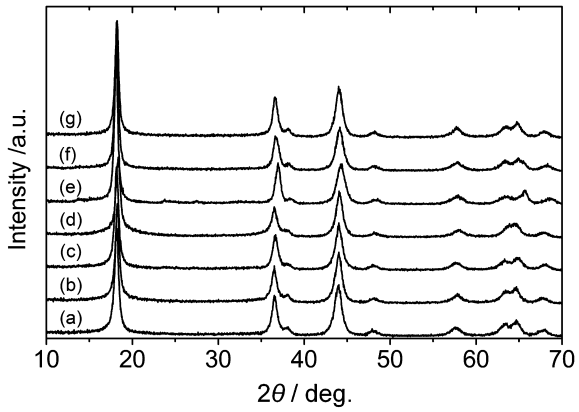

Fig. 1. XRD patterns for the $Li_{0.58}Na_{0.05}Mn_{0.56}Ni_{0.20}Ti_{0.24}O_2$ (a), $Li_{0.60}Na_{0.05}Mn_{0.62}Ni_{0.15}Ti_{0.23}O_2$ (b), $Li_{0.61}Na_{0.05}Mn_{0.67}Ni_{0.10}Ti_{0.23}O_2$ (c), $Li_{0.62}Na_{0.05}Mn_{0.72}Ni_{0.05}Ti_{0.23}O_2$ (d), $Li_{0.59}Na_{0.03}Mn_{0.91}Ni_{0.05}Ti_{0.04}O_2$ (e), $Li_{0.61}Na_{0.03}Mn_{0.82}Ni_{0.10}Ti_{0.08}O_2$ (f) and $Li_{0.60}Na_{0.03}Mn_{0.72}Ni_{0.15}Ti_{0.13}O_2$ (g).

Table 1
Chemical compositions and lattice parameters of $Li_xMn_yTi_zNi_{1-y-z}O_2$.

Sample	Composition determined by ICP	Lattice parameter	
		a (Å)	*c* (Å)
MNT552025	$Li_{0.58}Na_{0.05}Mn_{0.56}Ni_{0.20}Ti_{0.24}O_2$	2.883(5)	14.46(3)
MNT601525	$Li_{0.60}Na_{0.05}Mn_{0.62}Ni_{0.15}Ti_{0.23}O_2$	2.886(6)	14.40(3)
MNT651025	$Li_{0.61}Na_{0.05}Mn_{0.67}Ni_{0.10}Ti_{0.23}O_2$	2.878(6)	14.46(4)
MNT700525	$Li_{0.62}Na_{0.05}Mn_{0.72}Ni_{0.05}Ti_{0.23}O_2$	2.885(4)	14.33(2)
MNT900505	$Li_{0.59}Na_{0.03}Mn_{0.91}Ni_{0.05}Ti_{0.04}O_2$	2.854(13)	14.44(8)
MNT801010	$Li_{0.61}Na_{0.03}Mn_{0.82}Ni_{0.10}Ti_{0.08}O_2$	2.872(6)	14.47(4)
MNT701515	$Li_{0.60}Na_{0.03}Mn_{0.72}Ni_{0.15}Ti_{0.13}O_2$	2.878(6)	14.42(4)

capacity from 310 mAh g^{-1} to 267 mAh g^{-1} with increasing nickel contents, their samples increased the capacity retention rates. The initial discharge capacities of MNT900505, MNT801010 and MNT701515 samples decreased from 298 mAh g^{-1} to 283 mAh g^{-1} with the increasing the sum of nickel and titanium contents. The discharge curves gradually changed to be concave down in titanium-rich samples: MNT552025, MNT601525, MNT651025, MNT700525 and MNT701515. As shown in Fig. 3, Li/$Li_{0.6}Mn_{0.82}Ni_{0.10}Ti_{0.08}O_2$ (MNT801010) cell shows a better capacity retention rate of 87% after 20 electrochemical cycles than those of the other $Li_xMn_yNi_zTi_{1-y-z}O_2$ samples in that voltage range, where only a slight increase in a 4 V region was observed in discharge curves. The superior capacity retention and simple discharge profiles in MNT801010 cell might be attributed to the titanium contents of 0.08 molar ratio because the incorporation of Ti^{4+} in the O_3-type

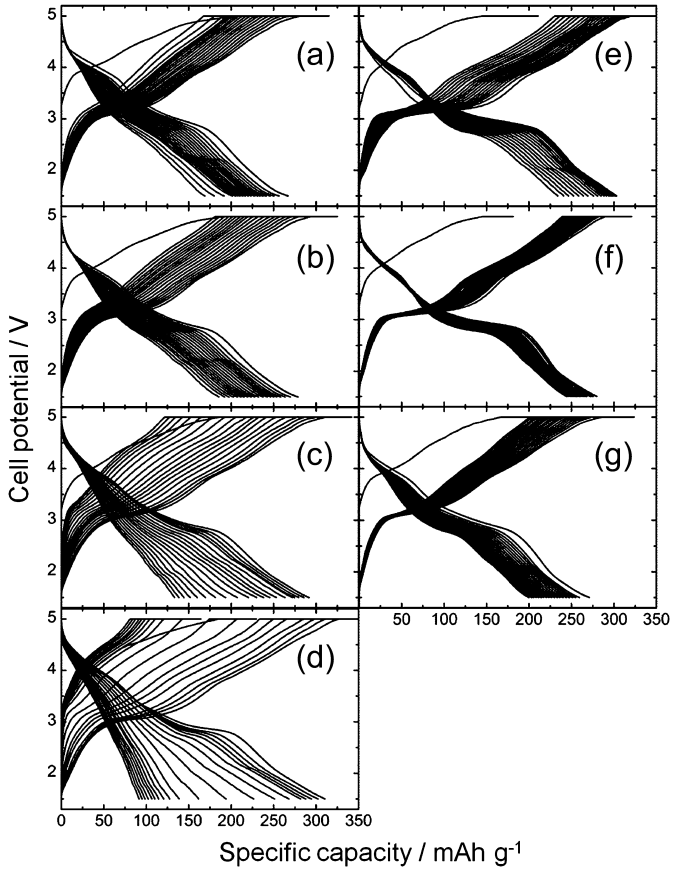

Fig. 2. Charge/discharge curves of the Li/$Li_xMn_yNi_zTi_{1-y-z}O_2$ ($x < 0.7$, $0.5 < y < 0.95$, $0.05 \le z < 0.25$) cells in the potential range between 1.5 and 5.0 V (30 mA g^{-1}) during 20 cycles: $Li_{0.58}Na_{0.05}Mn_{0.56}Ni_{0.20}Ti_{0.24}O_2$ (a), $Li_{0.60}Na_{0.05}Mn_{0.62}Ni_{0.15}Ti_{0.23}O_2$ (b), $Li_{0.61}Na_{0.05}Mn_{0.67}Ni_{0.10}Ti_{0.23}O_2$ (c), $Li_{0.62}Na_{0.05}Mn_{0.72}Ni_{0.05}Ti_{0.23}O_2$ (d), $Li_{0.59}Na_{0.03}Mn_{0.91}Ni_{0.05}Ti_{0.04}O_2$ (e), $Li_{0.61}Na_{0.03}Mn_{0.82}Ni_{0.10}Ti_{0.08}O_2$ (f) and $Li_{0.60}Na_{0.03}Mn_{0.72}Ni_{0.15}Ti_{0.13}O_2$ (g).

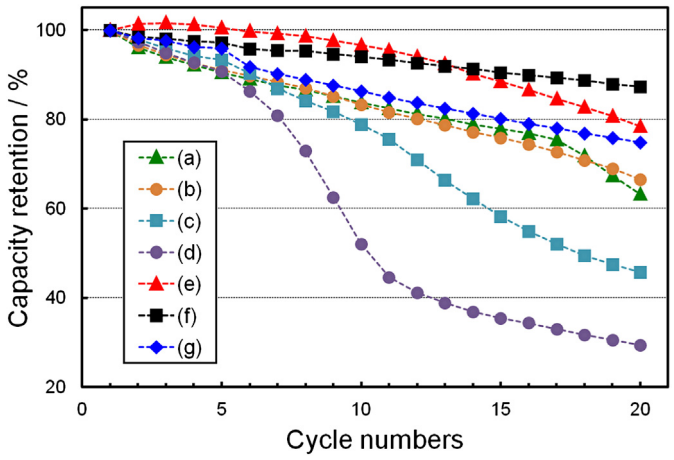

Fig. 3. Cycle performance of $Li_{0.58}Na_{0.05}Mn_{0.56}Ni_{0.20}Ti_{0.24}O_2$ (a), $Li_{0.60}Na_{0.05}Mn_{0.62}Ni_{0.15}Ti_{0.23}O_2$ (b), $Li_{0.61}Na_{0.05}Mn_{0.67}Ni_{0.10}Ti_{0.23}O_2$ (c), $Li_{0.62}Na_{0.05}Mn_{0.72}Ni_{0.05}Ti_{0.23}O_2$ (d), $Li_{0.59}Na_{0.03}Mn_{0.91}Ni_{0.05}Ti_{0.04}O_2$ (e), $Li_{0.61}Na_{0.03}Mn_{0.82}Ni_{0.10}Ti_{0.08}O_2$ (f) and $Li_{0.60}Na_{0.03}Mn_{0.72}Ni_{0.15}Ti_{0.13}O_2$ (g).

structure enhanced the chemical diffusivity in $LiNi_{0.5}Mn_{0.5-x}Ti_xO_2$ with $x = 0.05$ and 0.10 [11]. The stronger bond of Ti–O could accommodate the Jahn–Teller distortion around nickel or manganese ions. It would be supposed that there is appropriate titanium content to improve the electrochemical property. The physical properties affected by transition metals will be the subject of further study.

Fig. 4 shows observed, calculated and difference patterns for Rietveld refinement from the XRD data using initial structure model of $Li_{0.55}Mn_{0.5}Ni_{0.25}Ti_{0.25}O_2$ [17]. The resultant *R*-values reached $R_{wp} = 13.60\%$ and $R_p = 10.02\%$, with a fit indicator of GOF = $R_{wp}/R_e = 1.29$. This result accorded with the observed XRD pattern and calculated XRD patterns well. The lattice parameters for the $Li_{0.6}Mn_{0.82}Ni_{0.10}Ti_{0.08}O_2$ were refined by the Rietveld refinement to be $a = 2.8771(4)$ Å, $c = 14.616(2)$ Å and $V = 104.77(2)$ $Å^3$.

Incorporation of extra lithium by chemical lithium insertion was possible and resulted in the $Li_{1.06}Mn_{0.82}Ni_{0.10}Ti_{0.08}O_2$ (MNT801010 + Li) determined by ICP-AES. The chemical formula of MNT801010 + Li could be regarded as $Li_{1.0}Mn_{0.82}Ni_{0.10}Ti_{0.08}O_2$ except for residual minor LiI contents. Fig. 5 shows observed, calculated and difference patterns for Rietveld refinement from the XRD data using initial structure model of $Li_{0.55}Mn_{0.50}Ni_{0.25}Ti_{0.25}O_2$ [17]. This XRD

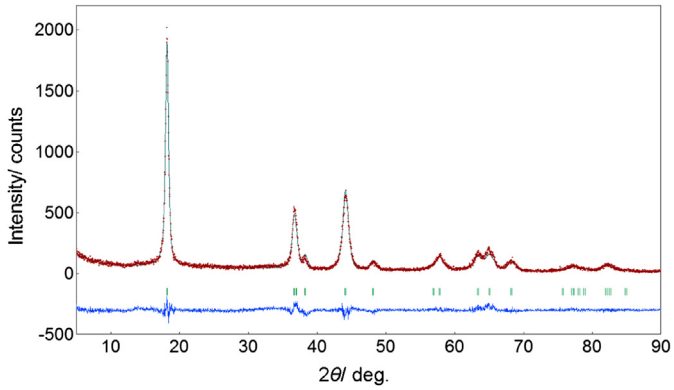

Fig. 4. Observed (red dot), calculated (solid dark green line) and difference plots (solid blue line) for the X-ray Rietveld analysis of the $Li_{0.6}Mn_{0.82}Ni_{0.10}Ti_{0.08}O_2$ synthesized by the Na^+/Li^+ ion exchange reaction. (For interpretation of the references to color in this figure legend, the reader is referred to the web version of this article.)

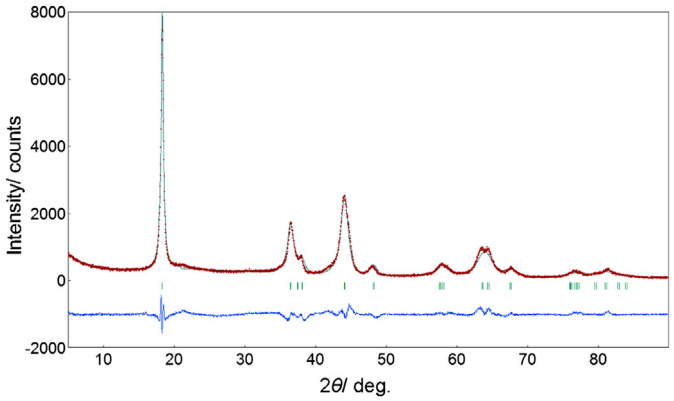

Fig. 5. Observed (red dot), calculated (solid dark green line) and difference plots (solid blue line) for the X-ray Rietveld analysis of the $Li_{1.0}Mn_{0.82}Ni_{0.10}Ti_{0.08}O_2$ synthesized by the chemical lithium insertion. (For interpretation of the references to color in this figure legend, the reader is referred to the web version of this article.)

data was collected for 5 s at each step due to the weak diffraction peaks. The resultant *R*-values reached $R_{wp} = 10.94\%$ and $R_p = 8.27\%$, with a fit indicator of GOF $= R_{wp}/R_e = 2.21$. This result accorded with the observed XRD pattern and calculated XRD patterns. The lattice parameters for the $Li_{1.0}Mn_{0.82}Ni_{0.10}Ti_{0.08}O_2$ were refined by the Rietveld refinement to be $a = 2.9067(5)$ Å, $c = 14.487(1)$ Å and $V = 106.00(3)$ Å^3. The shortened *c* axis after chemical lithium insertion implies that the inserted lithium ions were located in lithium site and attracted to the transition metal layers. The obtained powders were consisted of submicron particles and showed no change in morphology after chemical lithium insertion (Fig. 6).

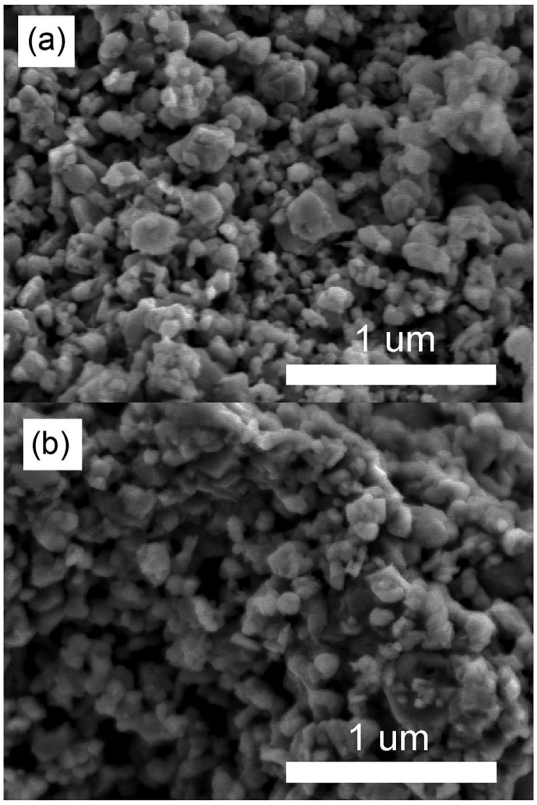

Fig. 6. SEM images for (a) Na^+/Li^+ ion-exchanged $Li_{0.6}Mn_{0.82}Ni_{0.10}Ti_{0.08}O_2$ and (b) chemically lithium inserted $Li_{1.0}Mn_{0.82}Ni_{0.10}Ti_{0.08}O_2$.

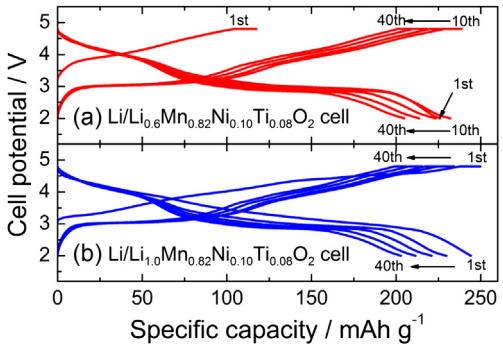

Fig. 7. Charge/discharge curves of the $Li/Li_{0.6}Mn_{0.82}Ni_{0.10}Ti_{0.08}O_2$ cell (a) and the $Li/Li_{1.0}Mn_{0.82}Ni_{0.10}Ti_{0.08}O_2$ cell (b) in the potential range between 2.0 and 4.8 V (30 mA g^{-1}) during 40 cycles.

Fig. 7 shows the charge and discharge curves of $Li/Li_{0.6}Mn_{0.82}Ni_{0.10}Ti_{0.08}O_2$ cell (a) and $Li/Li_{1.0}Mn_{0.82}Ni_{0.10}Ti_{0.08}O_2$ cell (b) from the 1st to 40th cycle operated at 30 mA g^{-1} in the voltage between 2.0 and 4.8 V. Open-circuit voltages (OCVs) of the above two cells were around 3.3 V (a) and 3.0 V (b) respectively. The lower OCV of the cell using chemical lithium inserted material (MNT801010 + Li) indicates that the transition metal ions in MNT801010 sample were reduced by the LiI treatment, $E^0 \approx 3.0$ V vs. Li/Li^+ [24]. After chemical lithium insertion, the first charge/discharge capacities increased from 144/225 mAh g^{-1} for MNT801010 to 250/244 mAh g^{-1} for MNT801010 + Li, which corresponds to deinsertion/insertion of 0.87/0.85 lithium atoms per formula unit (apfu). The $Li/Li_{1.0}Mn_{0.82}Ni_{0.10}Ti_{0.08}$ cell exhibited the irreversible capacity of ca. 6 mAh g^{-1} and the excellent coulombic efficiency of 98% (Fig. 8). The coulombic efficiency decreased to 96% at 2nd cycle and returned at 9th cycle followed by the constant efficiency of 98% (9th–40th). Although the irreversible capacities during cycling were mainly due to electrolyte oxidation occurring at about 4.5 V, rechargeable capacities more than 200 mAh g^{-1} after 40 cycles were obtained for the both cells using the electrode materials with and without chemical lithium insertion (Fig. 7).

This paper describes the performance of the graphite(C)/$Li_{1.0}Mn_{0.82}Ni_{0.10}Ti_{0.08}$ cell, i.e. full cell (Fig. 9). The first charge/discharge capacity was 247/208 mAh g^{-1} at 30 mA g^{-1} between 1.8 and 4.7 V. Although the first charge capacity was almost the same as lithium anode cell (250 mAh g^{-1}), the discharge one decreased from 244 mAh g^{-1} for a lithium cell to 208 mAh g^{-1} for a full cell. The large irreversible capacity loss, 39 mAh g^{-1}, was observed and common for a full-cell configuration with graphite anode and

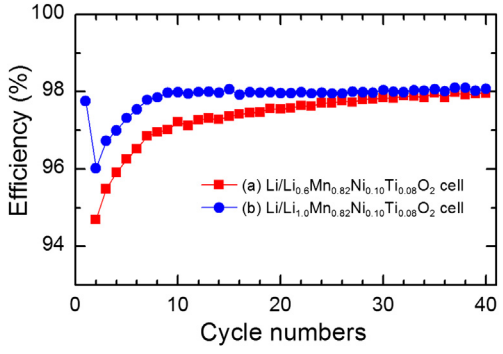

Fig. 8. Coulombic efficiency versus cycle numbers for $Li/Li_{0.6}Mn_{0.82}Ni_{0.10}Ti_{0.08}O_2$ cell (red line) and $Li/Li_{1.0}Mn_{0.82}Ni_{0.10}Ti_{0.08}O_2$ cell (blue line). (For interpretation of the references to color in this figure legend, the reader is referred to the web version of this article.)

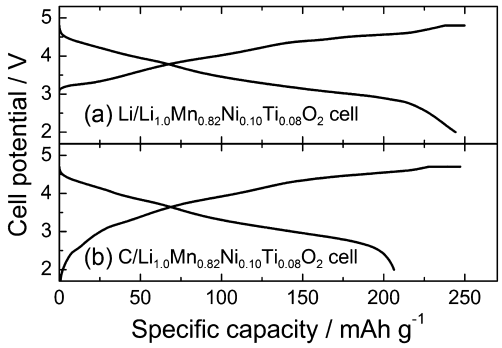

Fig. 9. First charge/discharge curves of the $Li/LiMn_{0.82}Ni_{0.10}Ti_{0.08}O_2$ cell (a) and the $C/LiMn_{0.82}Ni_{0.10}Ti_{0.08}O_2$ cell (b) in the potential range between 2.0 and 4.8 V for Li anode and 1.8 and 4.7 V for graphite (C) anode.

ascribed to be due to the utilization for the solid–electrolyte interface (SEI) formation [10]. The charge/discharge capacity of 247/208 mAh g^{-1} for the full cell corresponded to Li deinsertion/insertion of 0.87 apfu and 0.72 apfu. Since the lithium ion contents in Na^+/Li^+ ion-exchanged materials were below 0.72 apfu, the chemically inserted lithium ions of 0.15 apfu could be electrochemically intercalated or deintercalated in O_3-type $Li_{1.0}Mn_{0.82}Ni_{0.10}Ti_{0.08}O_2$ structure. Therefore the chemical insertion of lithium ions to positive electrode materials enabled to increase the electrochemical capacity especially for the graphite anode cell.

4. Conclusion

The novel materials with layered rock-salt type structure, $Li_xMn_yNi_zTi_{1-y-z}O_2$ ($x \leq 1.0$, $0.5 < y < 0.95$, $0.05 \leq z \leq 0.20$), were prepared by Na^+/Li^+ ion-exchange reaction and chemical lithium insertion. After Na^+/Li^+ ion-exchange reaction for the precursors, $Na_{0.7}Mn_yNi_zTi_{1-y-z}O_2$, all phases were identified as a layered rock-salt (O3) type structure with space group of $R\bar{3}m$. The electrochemical property shows that the highest capacity retention rate of all samples was obtained in $Li/Li_{0.6}Mn_{0.82}Ni_{0.10}Ti_{0.08}O_2$ cell. Chemical lithium insertion was carried out for the $Li_{0.6}Mn_{0.82}Ni_{0.10}Ti_{0.08}O_2$ sample to result in the layered rock-salt type $Li_{1.0}Mn_{0.82}Ni_{0.1}Ti_{0.08}O_2$. The lithium ions by chemically inserted were enabled to increase the electrochemical capacity especially for the graphite anode cell. The excellent initial coulombic efficiency of 98% was achieved for $Li/Li_{1.0}Mn_{0.82}Ni_{0.1}Ti_{0.08}O_2$ cell. Since the graphite(C)/$Li_{1.0}Mn_{0.82}Ni_{0.1}Ti_{0.08}O_2$ cell exhibited over 200 mAh g^{-1}, the present $Li_{1.0}Mn_{0.82}Ni_{0.1}Ti_{0.08}O_2$ material is one of the promising materials for positive electrode material in lithium ion batteries for the view point of high capacity and coulombic efficiency.

Acknowledgments

This study was supported financially by a national project (Li-EAD project) of the Ministry of Economy, Trade and Industry (METI) and the New Energy and Industrial Technology Development Organization (NEDO).

References

[1] K. Mizushima, P.C. Jones, P.J. Wiseman, J.B. Goodenough, Mater. Res. Bull. 15 (1980) 783–789.
[2] T. Ohzuku, A. Ueda, M. Nagayama, Y. Iwakoshi, H. Komori, Electrochim. Acta 38 (1993) 1159–1167.
[3] Y. Makimura, T. Ohzuku, J. Power Sources 119–121 (2003) 156–160.
[4] F. Capitaine, P. Gravereau, C. Delmas, Solid State Ionics 89 (1996) 197–202.
[5] A.R. Armstrong, P.G. Bruce, Nature 381 (1996) 499–500.
[6] A.R. Armstrong, A.J. Paterson, A.D. Robertson, P.G. Bruce, Chem. Mater. 14 (2002) 710–719.
[7] P. Strobel, B. Lambert-Andron, J. Solid State Chem. 75 (1988) 90–98.
[8] M.H. Rossouw, M.M. Thackeray, Mater. Res. Bull. 26 (1991) 463–473.
[9] M.M. Thackeray, S.H. Kang, C.S. Johnson, J.T. Vaughey, R. Benedek, S.A. Hackney, J. Mater. Chem. 17 (2007) 3112–3125.
[10] M. Tabuchi, Y. Nabeshima, T. Takeuchi, H. Kageyama, K. Tatsumi, J. Akimoto, H. Shibuya, J. Imaizumi, J. Power Sources 196 (2011) 3611–3622.
[11] S.-T. Myung, S. Komaba, K. Hosoya, N. Hiroaki, Y. Miura, N. Kumagai, Chem. Mater. 17 (2005) 2427–2435.
[12] T.A. Arunkumar, Y. Wu, A. Manthiram, Chem. Mater. 19 (2007) 3067–3073.
[13] S.-S. Shin, D.-W. Kim, Y.-K. Sun, Bull. Korean Chem. Soc. 23 (2002) 679–682.
[14] T.A. Eriksson, Y.J. Lee, J. Hollingsworth, J.A. Reimer, E.J. Cairns, X.-F. Zhang, M.M. Doeff, Chem. Mater. 15 (2003) 4456–4463.
[15] S. Patoux, M. Dolle, M.M. Doeff, Chem. Mater. 17 (2005) 1044–1054.
[16] P. Suresh, A.K. Shukla, N. Munichandraiah, Electrochem. Solid State Lett. 8 (2005) A263–A266.
[17] N. Ishida, H. Hayakawa, J. Akimoto, H. Shibuya, J. Imaizumi, Key Eng. Mater., in press.
[18] N. Ishida, H. Hayakawa, H. Shibuya, J. Imaizumi, J. Akimoto, Chem. Lett. 41 (2012) 1478–1480.
[19] B. Ammundsen, J. Paulsen, Adv. Mater. 13 (2001) 943–956.
[20] S.H. Park, Y.-K. Sun, C.S. Yoon, C.-K. Kim, J. Prakash, J. Mater. Chem. 12 (2002) 3827–3831.
[21] K.M. Shaju, G.V. Subba Rao, B.V.R. Chowdari, Electrochem. Commun. 4 (2002) 633–638.
[22] N. Ishida, H. Hayakawa, H. Shibuya, J. Imaizumi, J. Akimoto, J. Electrochem. Soc. (2013) A297–A301.
[23] F. Izumi, K. Momma, Proceedings of XX Conference Applied Crystallography, Solid State Phenom. 130 (2007) 15–20.
[24] J.M. Tarascon, D. Guyomard, J. Electrochem. Soc. 138 (1991) 2864–2868.